DOI: 10.2352/ISSN.2470-1173.2016.2.VIPC-229

Haze Removal of Single Remote Sensing Image by Combining Dark Channel Prior with Superpixel

Yanlin Tian, Chao Xiao, Xiu Chen, Daiqin Yang and Zhenzhong Chen; School of Remote Sensing and Information Engineering, Wuhan University; Wuhan, China

Abstract

Dehazing is important in remote sensing image restorations to enhance the acquired low quality image for interpretation. However, traditional methods have some limitations for dehazing of remote sensing images due to its color distortion and noise. In this paper, we propose an improved method combining superpixel segmentation with luminance information of a haze image to estimate the atmospheric light instead of dark channel prior. Using this method with the haze imaging model, we can directly estimate the thickness of the haze and restore a high quality haze-free image. Experimental results on a variety of remote sensing haze images demonstrate our approach can achieve better image quality when compared with well-known He's [1] method for remote sensing images.

Index Terms- Haze removal; superpixel segmentation; atmospheric scattering model;

I. INTRODUCTION

Suspended particles in the air (fog, impurities, smoke, etc.) cause atmospheric absorption and scattering, which degrade the quality of captured outdoor natural images. Thus, the images of outdoor scenes often have the problem, which includes low contrast, color distortion, and blurred minutiae. Haze removal (or dehazing) has been an important research topic. The restored haze-free image is more visually pleasing, and plays a better role in practical applications. Besides, most computer vision algorithms demand that the input image is the scene radiance. For example, in the case of monitoring traffic conditions under the foggy weather in the surveillance systems, haze-free images can better reflect the traffic flow and violations, which can provide a good basis for subsequent processing.

Haze removal has been a challenging problem. A number of researchers have carried out many in-depth researches and proposed different methods. At present, main methods of haze removal can be classified into two categories: (1) enhancement method based on image processing, (2) image restoration method based on a physical model. The latter is more persuasive, and closer to the imaging principle of images. Such methods can be divided into different sub-categories. Among them, the dehazing methods based on multiple images [2-6] (different weather conditions or different degree of polarization), are able to achieve a certain effect. But they have higher requirements to the input data, which is difficult to meet in most conditions. Using the method [7,8] of the known three-dimensional model to dehaze, also limits its usefulness. In recent years, single image haze removal [9] has made significant progresses. Tan [9] removes the haze by maximizing the local contrast of the restored image. The results are visually compelling but may not be physically valid. Fattal's approach [10] can also produce impressive results.

He's method has been well recognized [1], which uses dark channel prior to restore haze-free images. But there are still some limitations in some applications. When the colors of foreground are similar to the atmospheric light, the dehazing effect is not satisfactory. Moreover, the high computational complexity in the estimation of transmission limits the practical application of this approach.

In this paper, we propose an improved dehazing method for single remote sensing image which combines the haze imaging model and superpixel segmentation. In order to obtain more accurate atmospheric light, we transform the color space, and segment the image by using superpixel method, which divide the image into some regions (called superpixel) that consist of a series of pixels with similar color, luminance, texture and so on. When estimating the atmospheric light, traditional method, i.e., He's method [1], first pick the top 0.1% brightest pixels in the dark channel among which those with highest intensity in the input image is selected as the atmospheric light. It does not work well due to the color distortion and noise, as well as because the scene objects are inherently similar to the atmospheric light and no shadow is cast on them. In order to solve this problem, we calculate the mean luminance of a superpixel instead of a single pixel so that we can estimate atmospheric light more accurately and recover a hi-quality haze-free image. Furthermore, we reduce the computational complexity by ignoring the block effect when calculating the transmission due to its little influence on haze removal of remote sensing image.

The rest of this paper is organized as follows. In Section II, we introduce cultural background, including atmospheric scattering model, dark channel prior and normalized cut. Then we introduce our method and give detailed algorithm. Section III presents a quantitative comparison of our method to He's. Finally, we conclude in Section IV.

II. DEHAZING WITH SUPERPIXEL

This section briefly introduces the normalized cut [11-23] and dark channel prior. On this basis, we use atmospheric scattering model to process single remote sensing images under foggy (thin cloud) conditions. Then we give the detailed algorithm.

The framework of our proposed algorithm is shown in Fig. 1.

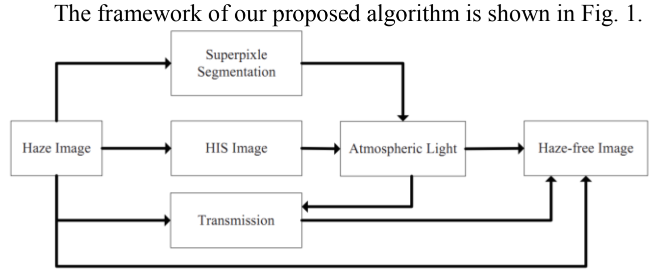

Figure 1. *Framework of our algorithm*

©2016 Society for Imaging Science and Technology
DOI: 10.2352/ISSN.2470-1173.2016.2.VIPC-229

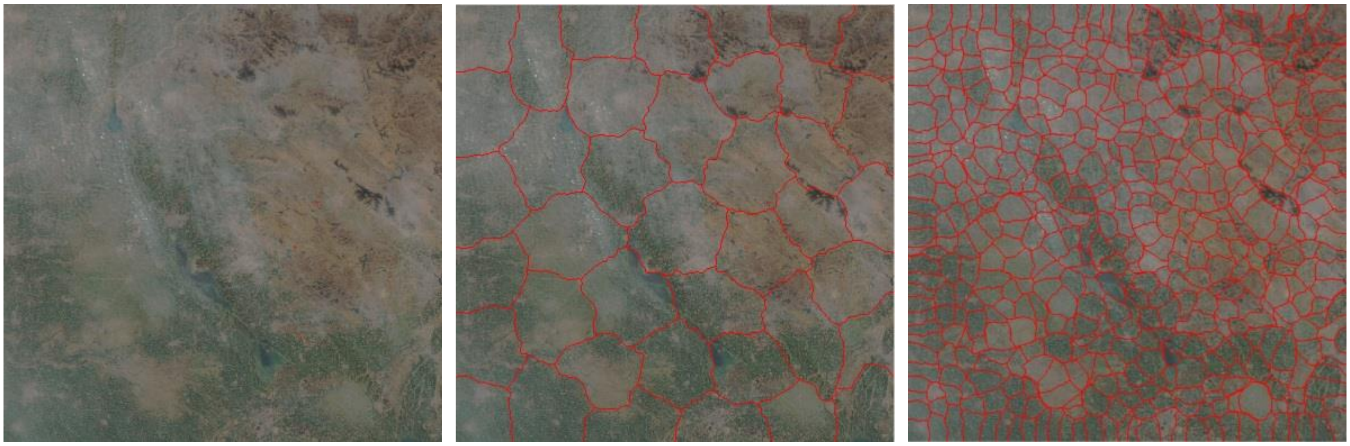

(a) (b) (c)

Figure 2. *Ncut results. (a) foggy image. (b) coarse segmentation result. (c) refined segmentation result.*

A. Atmospheric Scattering Model

In computer vision and computer graphics, the model widely used to describe the formation of a haze image is as follow:

$$I(x) = J(x)t(x) + A(1 - t(x)) \tag{1}$$

where I is the representative of remote sensing image under foggy weather. J represents haze-free image. A represents the value of atmospheric light. t is the transmittance. The dehazing process is to obtain J from the Eq. 1.

B. Estimation of Atmospheric Light

In natural images which contains region of the sky, atmospheric light is generally very close to the color of sky. At the same time the correlation between the luminance component of the haze image and atmospheric light is the largest. So we need to transform color space of the haze image to get the luminance information. In the color space of HIS, I, H and S represent luminance, hue and saturation respectively. I component is independent of H component and S component.

In addition to the color space transformation, we perform superpixel segmentation to process the haze image, so as to estimate atmospheric light more accurately.

Normalized cut (Ncut) [7] takes a picture as undirected graph, G = {V,E,W}, where V is a vertex set of the image, E is the set of all edges of the image, W is edge weights set of the image. By recursion method undirected graph is divided into two no intersection set A and B, and the union of two set is an undirected graph.

$$Ncut(A,B) = \frac{cut(A,B)}{assoc(A,V)} + \frac{cut(A,B)}{assoc(B,V)} \tag{2}$$

where cut(A, B) is A, B two sub-graphs cut, which means the sum of edge weights of A and B sub-graph. assoc(A,V) represents the sum of connecting edge weights which connects the nodes of set A and all other nodes. assoc(B,V) represents nodes of set B to all other nodes connected edge weights.

In order to get the optimal segmentation effect, which means to get the minimum value of the Ncut. Solving the minimum Ncut problem can be converted to eigenvalue problems of Eq. 3.

$$(D - W)y = \lambda Dy \tag{3}$$

where D is the diagonal matrix whose elements is the degrees of vertex. W is the weight matrix between the edges.

Normalized cut can control the number of superpixels generated. The shape of sub-region obtained by Ncut is more structured, but its complexity is linear to image size. We combine normalized cut with luminance information of haze image to estimate the value of atmospheric light. Fig. 2 shows segmentation result by using Ncut.

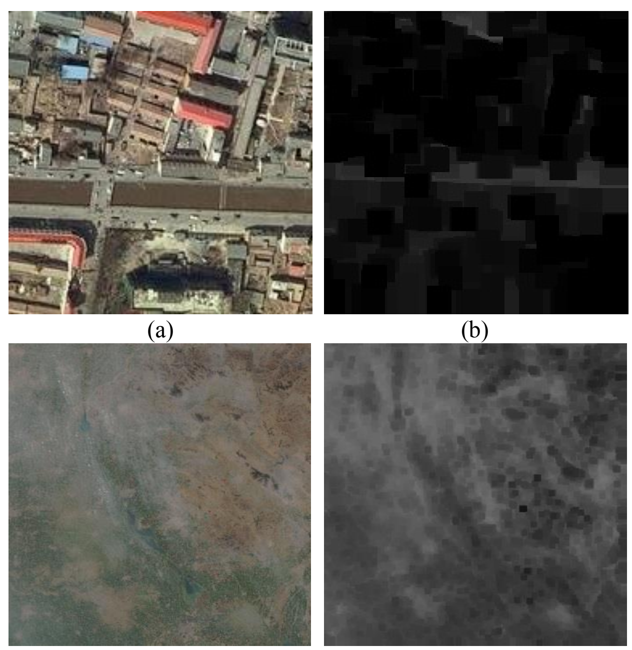

(a) (b)
(c) (d)

Figure 3. *remote sensing images and their dark channel image. (a) haze-free remote sensing image. (b) dark channel image of (a). (c) foggy remote sensing image. (d) dark channel image of (c).*

©2016 Society for Imaging Science and Technology
DOI: 10.2352/ISSN.2470-1173.2016.2.VIPC-229

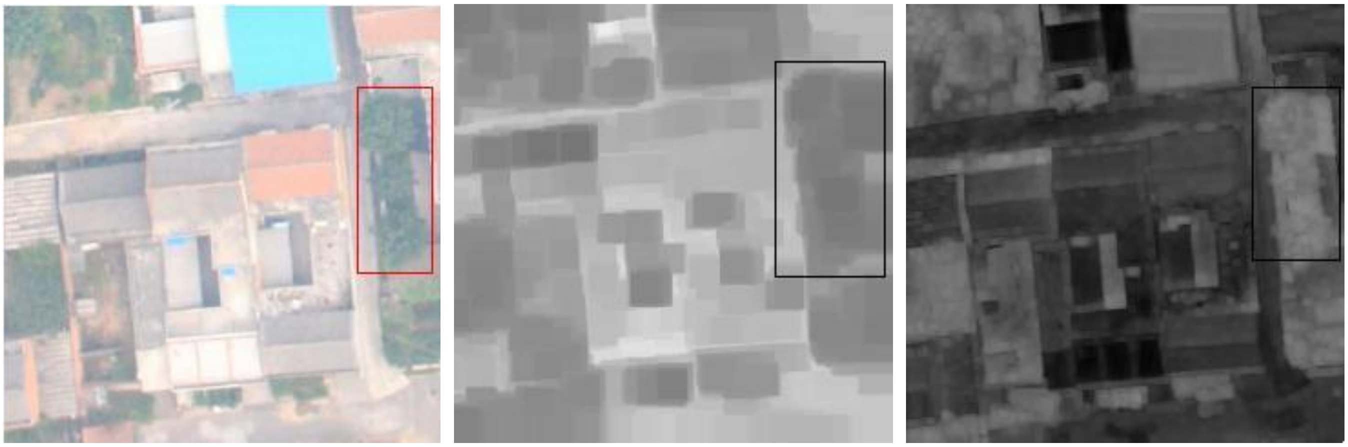

(a) (b) (c)

Figure 4. *block effect in dark channel image and transmission image. (a) foggy image. (b) dark channel image. (c) transmission map.*

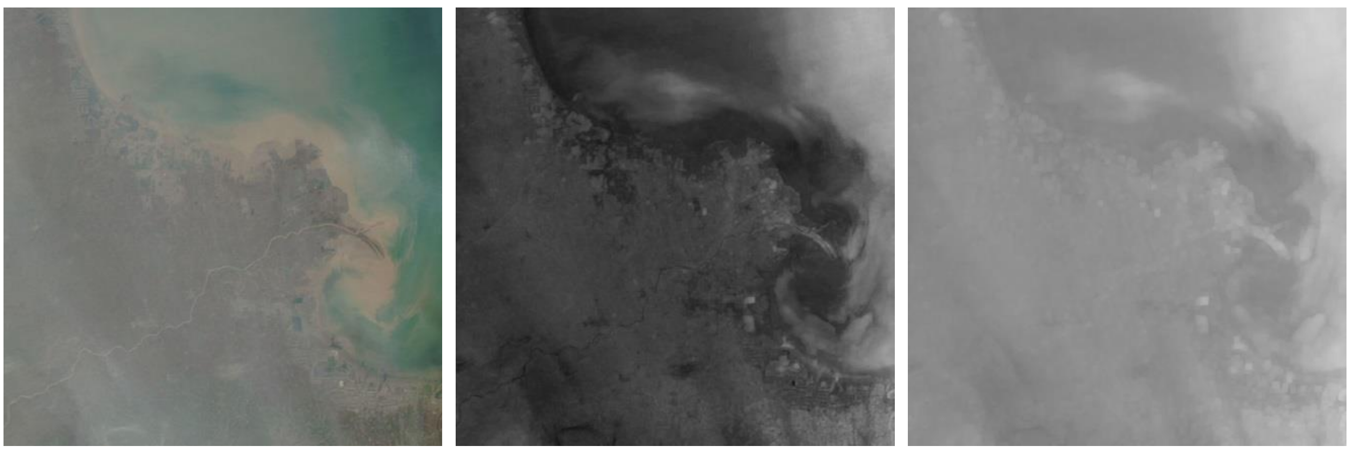

(a) (b) (c)

Figure 5. *transmission map obtained by our method and He's method. (a) foggy image. (b) our method. (c) He's method.*

C. Dark Channel Prior

The dark channel prior [1] is based on the statistics of the haze-free natural outdoor images. In most of the non-sky patches, at least one color channel has very low intensity at some pixels, or close to zero, these pixels are called dark pixels. In the foggy (thin cloud) images, these dark pixels is the main representative of atmospheric light. The empirical law is called the dark channel prior. For an image *J*:

$$J^{dark}(x) = \min_{c\in\{r,g,b\}}(\min_{y\in\Omega(x)}(J^{c}(y))) \tag{4}$$

where J^{C} is a color channel of *J*, and $\Omega(x)$ is a local patch centered at x. J^{dark} represents the dark channel of image *J*.

He [1] utilizes the dark channel prior to conduct the haze removal of natural images and achieves satisfactory results. We found that the dark channel prior is also applicable to remote sensing images from our research, i.e., the dark channel of haze-free remote sensing images has very low intensity. Here we present the dark channel images of a haze-free remote sensing image and a foggy remote sensing image in Fig. 3.

D. Estimating the Transmission

We assume that the transmission in a local patch $\Omega(x)$ is constant. Taking the min operation in the local patch and the min operation among three color channels on the Eq. 1, at the same time, applying dark channel prior of haze-free image to Eq. 1, we have estimated transmission as follow:

$$t(x) = 1 - \omega \min_{c}(\min_{y\in\Omega(x)}(\frac{I^{c}(y)}{A^{c}})) \tag{5}$$

where $\omega(0<\omega<1)$ is a constant parameter. c represents color channel. A is atmospheric light. The value of ω is application-based. We fix it to 0.95 for all results reported in this paper. The estimated transmission map obtained by using this method contains some block effects since the transmission is not always constant in a patch, but as can be seen in Fig. 4, the block effect has little effect on the remote sensing image, so in our method, the *t* in Eq. 5

©2016 Society for Imaging Science and Technology
DOI: 10.2352/ISSN.2470-1173.2016.2.VIPC-229

is set to the final transmission. From the results shown in Fig. 5, we can find that transmission map obtained by our method is darker than He's. That is to say, the atmospheric light in our method is smaller than He's. But from subsequent experiment results and quality assessment, it's clear that in remote sensing image without sky region, our method is more applicable to cope with it.

In summary, we make two improvements based on He's method [1]. First, we get luminance information of haze image combined Ncut to process the remote sensing haze image, and thus more accurately estimate the atmospheric light. Second, taking into account the characteristics of remote sensing image, and ignoring the impact of blocking effect to remote sensing images, thereby reducing the computational complexity in the estimation of transmission.

D. Algorithm Summary

As a summary, our proposed method consists of following steps:

1) Color space conversion is done in the remote sensing image, we transform the color space from RGB to HIS.

2) We first pick the top 0.1% brightest pixels in dark channel, and record the location of these pixels, using Ncut to segment the remote sensing image to generate the superpixels. Recorded locations are marked in superpixels. Thereafter we calculate the average of all pixels in every superpixel, the maximum average value is the estimation of atmospheric light A.

3) The method of calculating the rough transmittance used by He et al [1] using Eq. 5 is applied to the estimation of transmission of the remote sensing image.

4) According to Eq. 1, using the remote sensing image and the estimated value of A, t to obtain the dehazing remote sensing image.

III. EXPERIMENTAL RESULTS

We compare our method with He's method [1]. We objectively evaluate the quality of the dehazing remote sensing image. In our experiments, the patch size is set to 5×5 for each 800×800 image.

As shown from Figs. 6, 7 and 8, our approach can unveil the details and recover vivid color information where He's results still contain some fog in the image, which leads to the insufficient restoration of detailed features of the scenery. In dense haze regions, the dehazing effect of He's method is not remarkable. While our method makes restored haze-free image visually clearer, and have greater ability to dehaze.

In Tables 1, 2 and 3, we provide the evaluations based on Entropy and Average Gradient terms, where the greater entropy and average gradient, the better the quality of restored haze-free image. For Visible Edge Enhancement based on Contrast terms, greater e and r, smaller σ, better quality of restored haze-free image. As can be found from Tables 1 to 3, the quality of restored haze-free images by our method are improved in different degree. In terms of entropy, restored haze-free images by our method contain richer information than He's. As for average gradient, object edges in restored haze-free images by our method are clearer than that by He's.

From Table 1, we find in the relatively thin image the entropy of restored haze-free image by our approach increases by ten percent when compared to [1]. The average gradient of restored

Table 1: Results of Quality Evaluation of Images in Figure. 6.

	Entropy	Average Gradient	Visible Edge Enhancement		
			e	σ	r
Original image	11.9078	4.5145	-	-	-
He's method [1]	13.2974	5.8315	0.4776	0.001%	1.4071
Our method	14.5786	8.6546	0.8847	0.005%	2.1159

Table 2: Results of Quality Evaluation of Images in Figure. 7.

	Entropy	Average Gradient	Visible Edge Enhancement		
			e	σ	R
Original image	10.455	0.9808	-	-	-
He's method [1]	12.347	1.6071	4.2493	0	1.6166
Our method	12.6299	1.9465	13.375	0	2.2679

Table 3: Results of Quality Evaluation of Images in Figure. 8.

	Entropy	Average Gradient	Visible Edge Enhancement		
			e	σ	r
Original image	10.4016	1.5047	-	-	-
He's method [1]	12.1102	2.2203	1.9678	0	1.4254
Our method	12.7992	2.9672	8.7731	0	2.3075

haze-free image by our approach increases by 32 percent compared to [1]. The visible edge of restored haze-free image by ours is nearly twice that of He's. The number of saturated pixels is more than that obtained by He's. While in dense haze image, for example, in Fig.7, although the effect is not as good as Fig. 6, the quality of haze-free image from our method is better than the result from [1]. Especially, the number of saturated pixels is three times than that of [1].

In summary, our method outperform He's on haze removal of remote sensing image. Our method can not only get more distinct edge, but obtain richer texture information.

IV. CONCLUSION

In this paper, we have proposed an improved dehazing method. We utilize Ncut to estimate the atmospheric light instead of dark channel prior, which can better handle various difficult situations (e.g., when the scene objects are inherently similar to the atmospheric light, the dark channel prior will be invalid). Our experimental results have illustrated that the proposed method not only simplifies the estimation process of transmission in He's method [1], but also achieves better dehazing effect of remote sensing images. However, when there are a lot of dark areas in the input haze remote sensing images, dehazing performance of our algorithm still needs some improvements which would be our future work.

DOI: 10.2352/ISSN.2470-1173.2016.2.VIPC-229

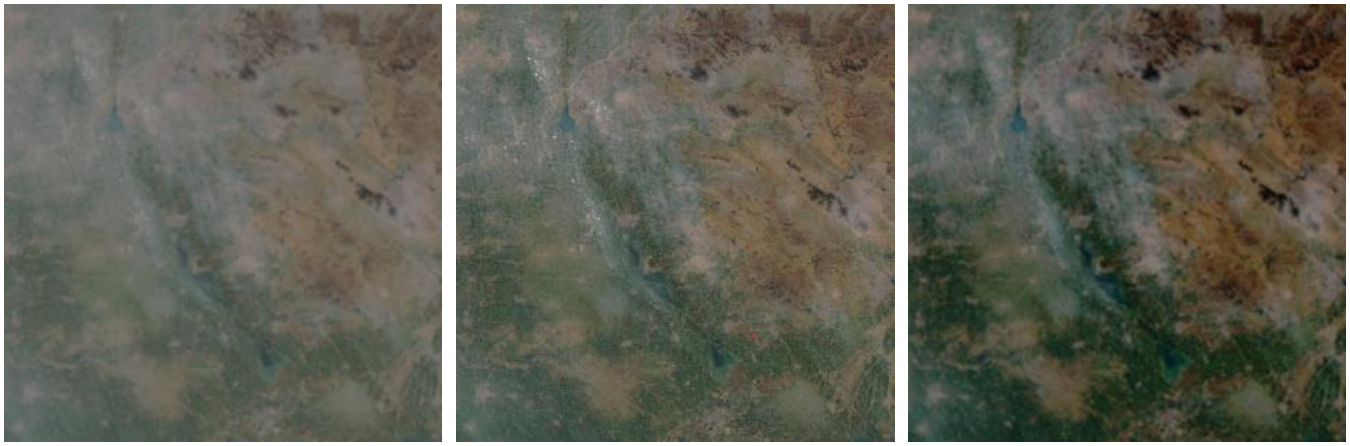

(a) (b) (c)

Figure 6. *Dehazing effect. (a) the input haze image. (b) image after haze removal by He's approach [1]. (c) image after haze removal by our approach.*

(a) (b) (c)

Figure 7. *Dehazing effect. (a) the input haze image. (b) image after haze removal by He's approach [1]. (c) image after haze removal by our approach.*

(a) (b) (c)

Figure 8. *Dehazing effect. (a) the input haze image. (b) image after haze removal by He's approach [1]. (c) image after haze removal by our approach.*

DOI: 10.2352/ISSN.2470-1173.2016.2.VIPC-229

IV. Acknowledgement

This work was supported in part by National Natural Science Foundation of China (No. 61471273, 91438203), National High-tech R&D Program of China (863 Program, 2015AA015903), and Natural Science Foundation of Hubei Province of China (No. 2015CFA053).

References

[1] K. He, J. Sun, and X. Tang, “Single image haze removal using dark channel prior,” IEEE Transactions on Pattern Analysis and Machine Intelligence, vol. 33, no. 12, pp. 2341-2353, 2011.

[2] Y. Y. Schechner, S. G. Narasimhan, and S. K. Nayar, “Instant dehazing of images using polarization,” in Proceedings of the 2011 IEEE Computer Society Conference on Computer Vision and Pattern Recognition, 2001. CVPR 2001. vol. 1. IEEE, 2001, pp. I-325.

[3] S. Shwartz, E. Namer, and Y. Y. Schechner, “Blind haze separation,” in 2006 IEEE Computer Society Conference on Computer Vision and Pattern Recognition, vol. 2. IEEE, 2006, pp. 1984-1991.

[4] S. G. Narasimhan, and S. K. Nayar. "Chromatic framework for vision in bad weather." In proceedings of IEEE Conference on Computer Vision and Pattern Recognition, 2000. Vol. 1. IEEE, 2000.

[5] S. G. Narasimhan, and S. K. Nayar. "Contrast restoration of weather degraded images." IEEE Transactions on Pattern Analysis and Machine Intelligence, 25.6 (2003): 713-724.

[6] S. K. Nayar, and S. G. Narasimhan. "Vision in bad weather." The Proceedings of the Seventh IEEE International Conference on Computer Vision, 1999. Vol. 2. IEEE, 1999.

[7] S. G. Narasimhan and S. K. Nayar, “Interactive (de) weather of an image using physical models,” in IEEE Workshop on Color and Photometric Methods in Computer Vision, vol. 6, no. 6.4. France, 2003, p. 1.

[8] J. Kopf, B. Neubert, B. Chen, M. Cohen, D. Cohen-Or, O. Deussen, M. Uyttendaele, and D. Lischinski. "Deep photo: Model-based photograph enhancement and viewing." ACM Transactions on Graphics (TOG). Vol. 27. No. 5. ACM, 2008.

[9] R. T. Tan, “Visibility in bad weather from a single image,” in IEEE Conference on Computer Vision and Pattern Recognition, 2008. CVPR 2008. IEEE, 2008, pp. 1-8.

[10] R. Fattal, “Single image dehazing,” in ACM Transactions on Graphics (TOG), vol. 27, no. 3. ACM, 2008, p. 72.

[11] X. Ren and J. Malik, “Learning a classification model for segmentation,” in Ninth IEEE International Conference on Computer Vision, 2003. Proceedings. IEEE, 2003, pp. 10-17.

[12] G. Mori, X. Ren, A. A. Efros, and J. Malik, “Recovering human body configurations: Combining segmentation and recognition,” in Proceedings of the 2004 IEEE Computer Society Conference on Computer Vision and Pattern Recognition, 2004. CVPR 2004. vol. 2. IEEE, 2004, pp. II-326.

[13] G. Mori, “Guiding model search using segmentation,” in Tenth IEEE International Conference on Computer Vision, 2005. ICCV 2005. vol. 2. IEEE, 2005, pp. 1417-1423.

[14] D. R. Martin, C. C. Fowlkes, and J. Malik, “Learning to detect natural image boundaries using local brightness, color, and texture cues,” IEEE Transactions on Pattern Analysis and Machine Intelligence, vol. 26, no. 5, pp. 530-549, 2004.

[15] J. Shi and J. Malik, “Normalized cuts and image segmentation,” IEEE Transactions on Pattern Analysis and Machine Intelligence, vol. 22, no. 8, pp. 888-905, 2000.

[16] R. Achanta, A. Shaji, K. Smith, A. Lucchi, P. Fua, and S. Susstrunk. "SLIC superpixels compared to state-of-the-art superpixel methods." IEEE Transactions on Pattern Analysis and Machine Intelligence, 34.11 (2012): 2274-2282.

[17] P. F. Felzenszwalb, and D. P. Huttenlocher. "Efficient graph-based image segmentation." International Journal of Computer Vision 59.2 (2004): 167-181.

[18] O. Veksler, Y. Boykov, and P. Mehrani, "Superpixels and supervoxels in an energy optimization framework." Computer Vision–ECCV 2010. Springer Berlin Heidelberg, 2010. 211-224.

[19] A. Vedaldi, and S. Soatto. "Quick shift and kernel methods for mode seeking." Computer Vision–ECCV 2008. Springer Berlin Heidelberg, 2008. 705-718.

[20] A. Levinshtein, A. Stere, K. N. Kutulakos, D. J. Fleet, S. J. Dickinson, and K. Siddiqi, "Turbopixels: Fast superpixels using geometric flows." IEEE Transactions on Pattern Analysis and Machine Intelligence, 31.12 (2009): 2290-2297.

[21] A. P.Moore, J. D. Prince, J. Warrell, U. Mohammed, and G. Jones, "Superpixel lattices." IEEE Conference on Computer Vision and Pattern Recognition, 2008. CVPR 2008. IEEE, 2008.

[22] M. Y. Liu, O. Tuzel, S. Ramalingam, and R. Chellappa, "Entropy rate superpixel segmentation." IEEE Conference on Computer Vision and Pattern Recognition, 2011. CVPR 2011, IEEE, 2011.

[23] J. Shotton, J. Winn, C. Rother, and A. Criminisi, "Textonboost for image understanding: Multi-class object recognition and segmentation by jointly modeling texture, layout, and context." International Journal of Computer Vision 81.1 (2009): 2-23.